Journal of Physics: Conference Series **708** (2016) 012003 doi:10.1088/1742-6596/708/1/012003

Unstable periodic orbits in plane Couette flow with the Smagorinsky model

Eiichi SASAKI[1], Genta KAWAHARA[1], Atsushi SEKIMOTO[2] and Javier JIMÉNEZ[2]

[1]Graduate School of Engineering Science, Osaka University, 1-3 Machikaneyama, Toyonaka, Osaka, Japan
[2]School of Aeronautics, U. Politécnica de Madrid, Madrid, Spain

E-mail: esasaki@me.es.osaka-u.ac.jp

Abstract. We aim at a description of the logarithmic velocity profile of wall turbulence in terms of unstable periodic orbits (UPOs) for plane Couette flow with a Smagorinsky-type eddy viscosity model. We study the bifurcation structure with respect to the Smagorinsky constant, arising from the gentle UPO reported by Kawahara and Kida [1] for the Navier-Stokes (NS) equation. We find that the obtained UPOs in the large eddy simulation (LES) system connect to those in the NS system, and that the gentle UPO in the LES system is an edge state branch whose stable manifold separates LES turbulence from an LES 'laminar' state. As the Reynolds number decreases this solution arises as the saddle solution of the saddle-node bifurcation. Meanwhile, the mean and root-mean-square velocity profiles of the node solution of the LES gentle UPO are in good agreement with those of LES turbulence.

1. Introduction

Near-wall turbulence can be found in daily life, which attracts many researchers' interests in the physical and engineering viewpoints, and its mean velocity has a well-known logarithmic profile that is considered the result of its multi-scale structure. Although there is a vast number of studies on near-wall turbulence, the dynamical origin of the logarithmic profile is not clear.

Plane Couette flow is one of the simplest shear flows, driven by parallel walls moving in opposite directions. Since the linear streamwise velocity profile of the laminar solution is linearly stable [2], there is no non-trivial solution bifurcating from the laminar one, and this problem is considered to be a typical example of subcritical transition to turbulence. Hamilton et al. [3] studied the minimal periodic domain where turbulence is sustained at low Reynolds numbers. In this domain, which we call the minimal flow unit [4] from now on, turbulence exhibits a quasi-periodic motion characterized by the formation and collapse of the streaks, i.e., the regeneration cycle. Kawahara and Kida [1] found two unstable periodic orbits (UPOs) in the minimal flow unit. Here we call them the vigorous and gentle UPOs. The vigorous UPO is embedded in turbulent state, its motion is characterized by the regeneration cycle, and the profiles of the mean and root-mean-square (RMS) velocities are similar to those of turbulence. On the other hand, the gentle UPO is an edge state that lies on the basin boundary between turbulent and laminar states. Other non-trivial solutions have been found, such as steady states [5, 6, 7], UPOs embedded in low-Reynolds-number turbulence [8] and localized solutions [9, 10], but all

the found solutions correspond to transitional or turbulent flows at low Reynolds numbers rather than fully developed high-Reynolds-number turbulence.

Our aim is to find an explanation of developed wall turbulence in terms of dynamical properties of invariant sets. In order to decrease the number of degrees of freedom, we introduce the Smagorinsky-type eddy viscosity model. Large-eddy simulation (LES) can reproduce not only the profile of the mean flow, but its dynamics are similar to Navier-Stokes (NS) turbulence. In the case of NS system, the invariant solution found by Kawahara and Kida [1] describes the dynamics of low-Reynolds-number NS turbulence, i.e. the regeneration cycle. When we introduce the eddy-viscosity model, several questions arise: for example, whether or not there are invariant solutions representing LES turbulence, and whether we can obtain descriptions of developed turbulence using those solutions even the small-scale motion is modelled by an eddy viscosity. Having the similar questions, Rawat et al. [11] showed an LES steady state which represents the large-scale motion in plane Couette flow. Here we study whether the eddy viscosity model changes the phase-space structure of the NS system, and explore the bifurcation structure stemming from the gentle UPO with respect to the Smagorinsky constant.

In section 2 we explain the problem setting and show bifurcation structure arising from the gentle UPO in section 3. The gentle UPO in the NS system continuously connects to the LES system and the LES gentle UPO is the edge state at low Reynolds numbers. Those results suggest that the eddy viscosity model does not violate a phase-space structure of the NS system. As the Reynolds number decreases we find the saddle-node bifurcation, and the node solution of the LES gentle UPO is embedded in turbulent state. The profiles of the mean and RMS velocities of this solution are similar to those of turbulence, although its dynamics is simpler than the regeneration cycle observed in turbulent state. Section 4 is devoted to the conclusion and discussion.

2. Problem setting

We deal with the dimensionless LES equation with the Smagorinsky model [12, 13] given by

$$\frac{\partial u_i}{\partial t} + u_j \partial_j u_i = -\partial_i p + 2\partial_j \left\{ \left(\frac{1}{Re} + \nu_e \right) S_{ij} \right\}, \tag{1}$$

$$\partial_i u_i = 0, \tag{2}$$

where t indicates time, $(u_1, u_2, u_3) = (u, v, w)$ is the velocity vector, and p is the kinematic pressure. Here $\partial_i = \partial/\partial x_i$ stands for the spacial derivative with respect to x_i and $S_{ij} = (\partial_i u_j + \partial_j u_i)/2$ is the strain rate tensor, where $(x_1, x_2, x_3) = (x, y, z)$ are the streamwise, wall-normal and spanwise coordinates, respectively. Quantities are normalized with the half-distance between walls, h, and the half-difference of the wall velocities, so that $Re = Uh/\nu$, where ν is the kinematic molecular viscosity. The dimensionless eddy viscosity ν_e is defined as

$$\nu_e = \{C_S \Delta(y) f_S(y)\}^2 |S|, \tag{3}$$

where $|S| = \sqrt{2 S_{ij} S_{ij}}$. Here C_S denotes the Smagorinsky constant, whose value is usually in the range of $0.1 \leq C_S \leq 0.15$, the filter width $\Delta(y) = \{\Delta_x \Delta_y(y) \Delta_z\}^{1/3}$ is defined from the grid spacings, and $f_S(y) = 1 - \exp(-y^+/A^+)$ is the van Driest damping function, with $A^+ = 25$. The $^+$ superscript denotes quantities rescaled with the friction velocity and the molecular viscosity. We impose periodic boundary conditions in the streamwise and spanwise directions, and the non-slip and impermeability conditions at the walls, $u|_{y=\pm 1} = \pm 1$ and $v|_{y=\pm 1} = w|_{y=\pm 1} = 0$. We set the streamwise and spanwise periods as the minimal flow unit, $L_x = 1.755\pi$, $L_z = 1.2\pi$ [3, 4].

We employ the Chebyshev-Fourier-Galerkin spectral method. For example, the wall-normal velocity is expanded as

$$v(x,y,z,t) = \sum_{k=-K}^{K} \sum_{l=-L}^{L} \sum_{m=0}^{M-4} \hat{v}_{k,l,m}(t) \exp(\mathrm{i}(\alpha k x + \beta l z)) \Psi_m(y), \tag{4}$$

where $\hat{v}_{k,l,m}(t)$ is the expansion coefficient, $(\alpha, \beta) = (2\pi/L_x, 2\pi/L_z)$ denote fundamental wavenumbers, and $\Psi_m(y)$ is the wall-normal Galerkin base defined by $\Psi_m(y) = T_m(y) - \frac{2m+4}{m+3} T_{m+2}(y) + \frac{m+1}{m+3} T_{m+4}(y)$, in terms of the m-th order Chebyshev polynomials, $T_m(y)$. Here K, L and M denote the truncation mode numbers, and we take the number of the grid points as $N_x \geq 3K+1, N_y = M+1, N_z \geq 3L+1$. In this paper, we set up the number of grid points and the truncation mode numbers as $(N_x, N_y, N_z) = (24, 33, 24)$ and $(K, L, M) = (7, 32, 7)$, respectively. The time integration is carried out using the second-order Crank–Nicholson and Adams–Bashforth methods. To obtain UPOs we employ the Newton-GMRES method. The periodic orbit with the period T is the solution of the equation,

$$\boldsymbol{\phi}_T(\boldsymbol{x}) - \boldsymbol{x} = \boldsymbol{0}, \tag{5}$$

where $\boldsymbol{x} \in \mathbb{R}^N (N = 2(2K+1)(2L+1)(M-2) + 2(M-1))$ is the N-dimensional real vector constructed by the real and imaginary parts of the expansion coefficients, and $\boldsymbol{\phi}_T(\boldsymbol{x})$ denotes the time-T map given by the time integration up to T from the initial condition $\boldsymbol{x}$. Substituting $\boldsymbol{x} = \boldsymbol{x}_0 + \delta\boldsymbol{x}$ and $T = T_0 + \delta T$ to (5) and linearizing the equations, we obtain

$$\left(\left. \frac{\partial \boldsymbol{\phi}}{\partial \boldsymbol{x}} \right|_{\boldsymbol{x}_0, T_0} - I \right) \delta\boldsymbol{x} + \boldsymbol{f}(\boldsymbol{x}_0) \delta T = -\boldsymbol{\phi}(\boldsymbol{x}_0)_{T_0} + \boldsymbol{x}_0, \tag{6}$$

where $\partial\boldsymbol{\phi}/\partial\boldsymbol{x}$ represents the monodromy matrix of the time-T map, I means the $N \times N$ identity matrix, and $\boldsymbol{f}(\boldsymbol{x})$ indicates the time derivative of $\boldsymbol{x}$. The linearized equation (6) has the N equations in the $N+1$ unknowns. Then, we consider the additional condition [14],

$$(\boldsymbol{f}(\boldsymbol{x}_0), \delta\boldsymbol{x}) = 0, \tag{7}$$

where $(\boldsymbol{x}, \boldsymbol{y})$ signifies the Euclidean inner product. To solve the equations (6) and (7), we carry out the GMRES computation [15], which is performed in the Krylov subspace without any inverse-matrix calculations. The stopping condition of the Newton iteration is

$$\frac{||\boldsymbol{\phi}_T(\boldsymbol{x}) - \boldsymbol{x}||}{||\boldsymbol{x}||} < 10^{-5}, \tag{8}$$

where $||\boldsymbol{x}|| = (\boldsymbol{x}, \boldsymbol{x})^{1/2}$ represents the Euclidean norm.

3. Bifurcation diagram of gentle UPO

Figure 1 shows the bifurcation structure arising from the gentle UPO reported by Kawahara and Kida [1] where the vertical axis indicates the maximal value of the cross flow energy defined by

$$E_{2\mathrm{D}} = \max_{t \in T} \int \frac{v^2 + w^2}{2} \frac{\mathrm{d}V}{2L_x L_z}. \tag{9}$$

In the case of $C_S = 0$, which represents the NS system, the gentle UPO is a saddle solution of the saddle-node bifurcation at $Re = 236.1$ [16]. As C_S increases the gentle UPO in the NS

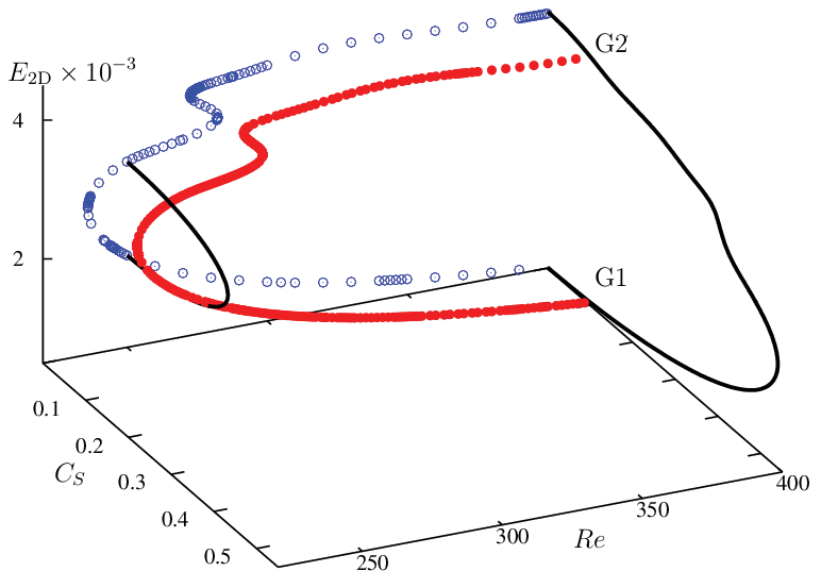

Figure 1. Bifurcation diagram of the gentle UPO. The vertical axis indicates the maximal value of the cross flow energy in the period. The blue and red points represent the cases of $C_S = 0$ (NS system) and 0.1, respectively. In the cases of $Re = 250$ and 400 the saddle-node bifurcation points are at $C_S = 0.2362$ and 0.5392, respectively.

system continuously connects with that in the LES system, and the branch finally reaches the node solution of the gentle UPO in the NS system through the saddle-node bifurcation at the finite C_S. In the case of $C_S = 0.1$, the gentle UPO appears from the saddle-node bifurcation at $Re = 238.4$. We have confirmed that the LES gentle UPO is also an edge state using the shooting method [17] (not shown). Hereafter we call the gentle UPO and the node solution G1 and G2, respectively.

In the case of $Re = 400$, the orbit projections on the total energy and the injection plane are shown in figure 2. Here the total energy E_{3D} and the injection I are given by

$$E_{3D} = \int \frac{u^2 + v^2 + w^2}{2} \frac{\mathrm{d}V}{2L_x L_z}, \tag{10}$$

$$I = \frac{1}{2}\left(\left.\frac{\mathrm{d}\langle u \rangle}{\mathrm{d}y}\right|_{y=+1} + \left.\frac{\mathrm{d}\langle u \rangle}{\mathrm{d}y}\right|_{y=-1} \right), \tag{11}$$

where $\langle\ \rangle$ denotes the wall-parallel averaging. The turbulent orbits and UPOs in the LES system do not change a lot from the NS systems. Those results suggest that the eddy viscosity model does not violate the phase-space structure of the NS system. Similar results are reported by Rawat et al. [11] in the case of the steady states.

G2 is embedded in the turbulent state. The mean and RMS velocities of G2 are shown in figure 3, while figure 4 presents the snapshot of the streamwise velocity. G2 has the three symmetries,

$$\Sigma_1 : (u, v, w)(x, y, z, t) \to (u, v, -w)(x + L_x/2, y, -z, t), \tag{12}$$

$$\Sigma_2 : (u, v, w)(x, y, z, t) \to (-u, -v, w)(-x, -y, z + L_z/2, t), \tag{13}$$

$$\Sigma_3 : (u, v, w)(x, y, z, t) \to (u, v, w)(x + L_x/2, y, z, t + T/2). \tag{14}$$

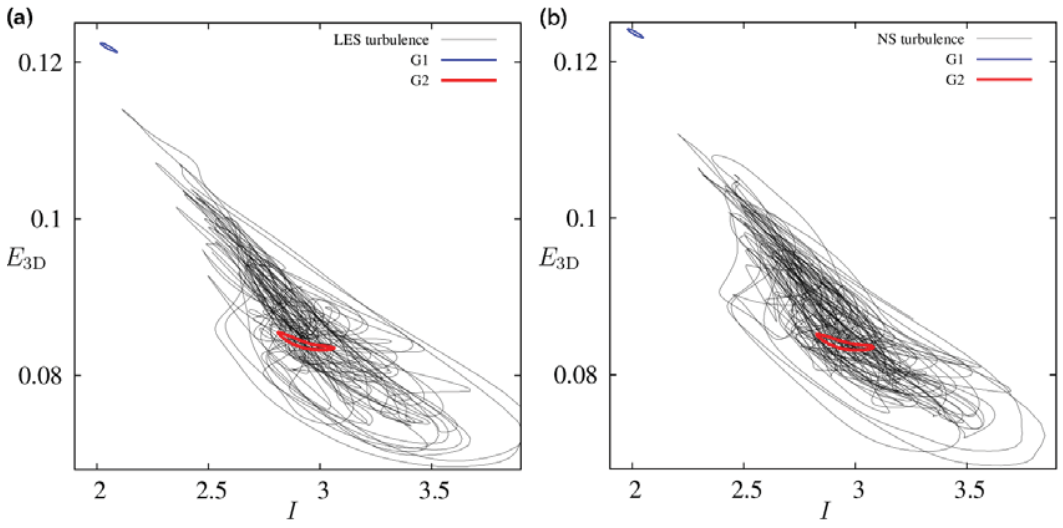

Figure 2. The projection on the total energy and the injection plane at $Re = 400$: (a) the LES ($C_S = 0.1$) and (b) the NS ($C_S = 0$) systems. The blue and red lines indicate G1 and G2, while the gray thin line means the turbulent orbit. In the case of the LES system, the periods of G1 and G2 are 84.13 and 63.23, respectively.

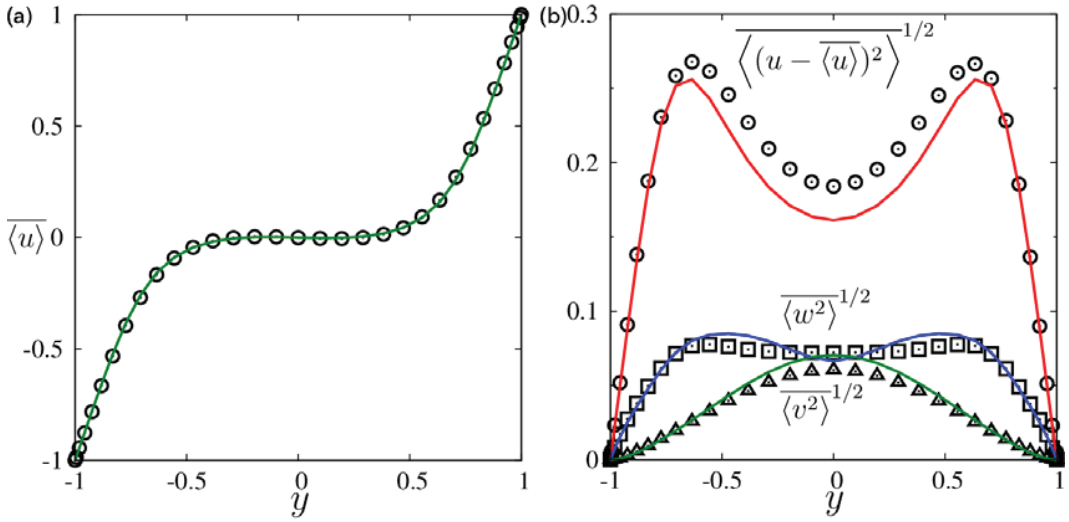

Figure 3. The mean velocity profiles of G2 at $C_S = 0.1$ and $Re = 400$: (a) the mean and (b) RMS velocities, where $\overline{\langle\ \rangle}$ signifies the time and the wall-parallel averaging. The symbols and lines denote the profiles of LES turbulence and G2, respectively.

The profiles of the mean and RMS velocities of G2 are similar to those of turbulence, but the dynamics is characterized only by a meandering of the streaks, which is simpler than the regeneration cycle, that is the formation and collapse of the low-speed streak found by Jiménez and Moin [4] and Hamilton et al. [3].

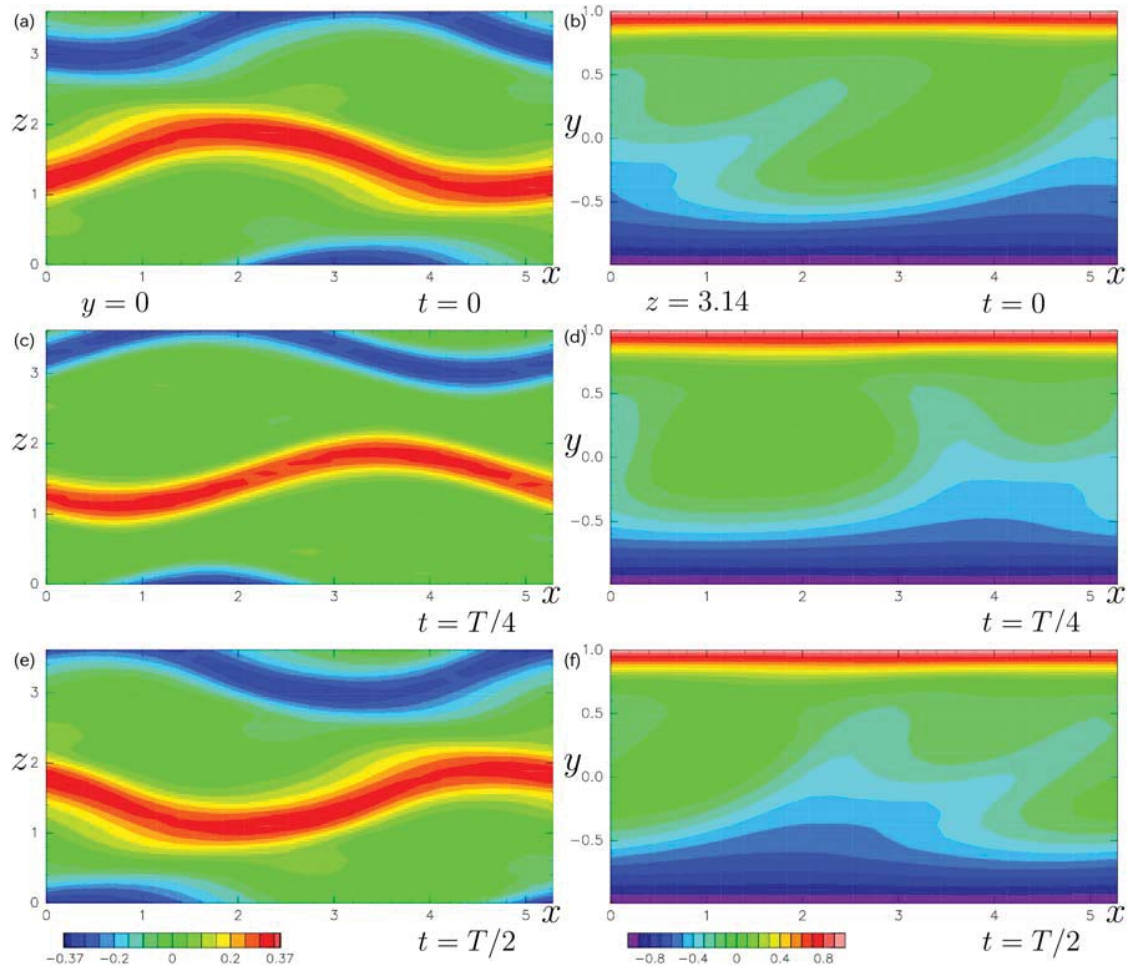

Figure 4. The time series of the streamwise velocity of G2 at $C_S = 0.1, Re = 400$. The left and right columns show the plane $y = 0$ and the plane $z = 3.14$, respectively. The top, middle and bottom rows show the snapshots at $t = 0, T/4$ and $T/2$, respectively.

4. Conclusion and discussion

We have studied the bifurcation structure arising from the gentle UPO found by Kawahara and Kida [1]. The gentle UPO is the edge state at $Re = 400$ in the NS system. We find that, as C_S increases, the gentle UPO of the NS system connects with the LES branch which reaches the node solution of the NS system through a saddle-node bifurcation at a finite Smagorinsky constant. In addition, the saddle solution in the LES system is also an edge state. Those results suggest that the eddy viscosity model would not violate the phase-space structure of the NS systems. Moreover the node solution is embedded in the turbulent state, and the profiles of the mean and RMS velocities are similar to those of turbulence. On the other hand, the dynamics of the node solution is represented only by a meandering motion of the streaks, which is simpler than the regeneration cycle. It should be noted that Kawahara and Kida [1] found a different vigorous UPO that describes the statistical and dynamical properties of turbulence. Since the magnitude of the eddy viscosity is small at the low Reynolds number $Re = 400$ as shown in figure A2 in the appendix, the LES contribution is not significant. At higher Reynolds numbers we are now tracing the corresponding LES branches to the node solution and the vigorous solution, which could represent high-Reynolds-number turbulence.

It is also an interesting problem to characterize the nonlinear stability of the laminar state at high Reynolds number in terms of a periodic edge state and its stable/unstable manifolds. Peixinho and Mullin [18] examined experimentally the transition to turbulence in pipe flow, and found that the minimal amplitude of the disturbance leading to turbulence changes as Re^{-m} with $m \approx 1.3-1.5$. Avila et al. [20] studied a transiently turbulent state, the so-called puff, and its characteristic lifetime. They found that the lifetime of this turbulent state is finite, which implies that perhaps the turbulent state at high Reynolds numbers might be a chaotic saddle in the dynamical systems theory. van Veen and Kawahara [19] showed the existence of the chaotic saddle using the homoclinic tangle arising from the gentle UPO at low Reynolds numbers.

Acknowledgments
The first author would like to thank Prof. Michio Yamada for fruitful discussions. This work was supported by JSPS KAKENHI Grant Number 50214672 and partially by the Multiflow program of the European Research Council.

Appendix A. Statistical properties of LES turbulence

Here we briefly show the statistical properties of LES turbulence ($C_S = 0.1$) at high Reynolds numbers in the minimal flow unit, $(L_x, L_z) = (1.755\pi, 1.2\pi)$, to check the validity of the eddy viscosity model. Time averaging is carried out integrating up to $T_\mathrm{e} = 4000$, after discarding an initial transient up to $T_\mathrm{e} = 2000$.

Figure A1 shows the mean streamwise velocity. As we increase the Reynolds number with a fixed number of grid points, $(N_x, N_y, N_z) = (24, 33, 24)$ the mean streamwise velocity moves closer to the laminar profile. On the other hand, if we change the number of the grid points for each Reynolds number, the mean velocity profile reproduces the same Kármán constant of NS turbulence, $\kappa \approx 0.41$ shown by Pirozzoli et al. [21]. It should be noted that because of the small domain size of and low Reynolds number of the present LES, one should expect deviations from the logarithmic profile of the NS system in the overlap region. In fact, we have confirmed a good agreement between the profile of the mean streamwise velocity of the LES and NS systems in the case of $(L_x, L_z) = (2\pi, \pi)$ (not shown). As the Reynolds number and the number of the grid points increase, the filter width near the wall changes as $\Delta(1)^+ \simeq 1.88, 6.31, 11.0$ and 9.63 for $Re = 400, 2000, 5000$ and 10000, respectively. Figure A1 then suggests that to obtain an approximately constant Kármán constant the grid should be taken so as to satisfy $\Delta(1)^+ \leq 10$. Taking into account the numerical costs to obtain UPOs using the Newton method we anticipate that the practical limitation of the Reynolds number using present resources would be in the range of $Re \leq 5000$.

Figure A2 shows the ratio $\overline{\langle \nu_e \rangle}/Re^{-1}$ of the mean eddy viscosity to the kinematic molecular one. As the Reynolds number increases the ratio increases monotonically except for the case of $Re = 10000$ where we not only change the number of wall-normal grid points but also the wall-parallel one. Even at high Reynolds numbers the order of magnitude is moderate, less than unity. This implies that the eddy viscosity model might not significantly change the energy dissipation mechanism of the NS system. It should be noted that since the eddy viscosity is small at $Re = 400$, the LES contribution is unimportant at this low Reynolds number.

References

[1] Kawahara G and Kida S 2001 *J. Fluid Mech.* **449** 291–300
[2] Romanov V A 1973 *Funct. Anal. Appl.* **7** 137–146
[3] Hamilton J M, Kim J and Waleffe F 1995 *J. Fluid Mech.* **287** 317–348
[4] Jiménez J and Moin P 1991 *J.Fluid Mech.* **225** 213–240
[5] Nagata M 1990 *J. Fluid Mech.* **217** 519–27
[6] Wang J, Gibson J and Waleffe F 2007 *Phys. Rev. Lett.* **98** 204501
[7] Itano T, Akinaga T, Generalis S C and Seki M S 2013 *Phys. Rev. Lett.* **111** 184502

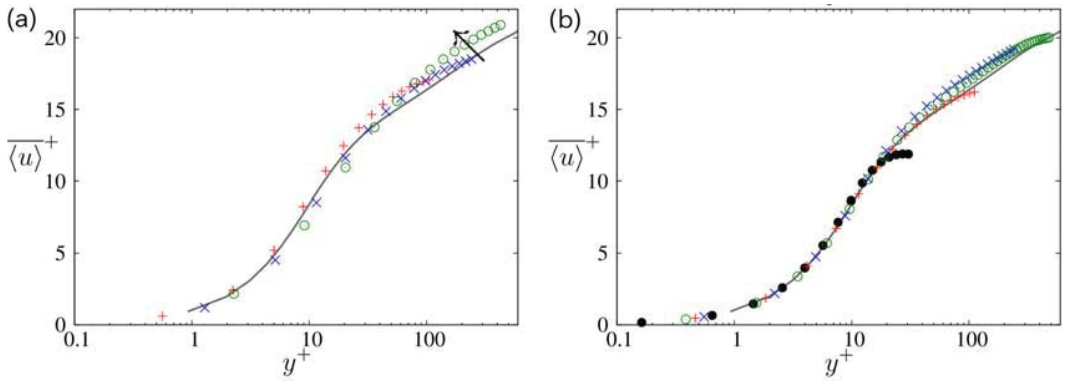

Figure A1. Mean streamwise velocity at several Reynolds numbers: ● , $Re = 400$; +, 2000; ×, 5000; ○ , 10000. (a) The number of the grid points is fixed to $(N_x, N_y, N_z) = (24, 33, 24)$. (b) Grid increases with the Reynolds number. $(N_x, N_y, N_z) = (24, 33, 24), (24, 37, 24), (24, 49, 24)$ and $(48, 81, 48)$, where $h^+ = 33.7, 122, 258$ and 503, respectively. The gray line shows the result of a DNS of plane Couette flow in a periodic domain $(L_x, L_z) = (18\pi, 8\pi)$ at $h^+ = 550$ [22] We note that the profile at $Re = 400$ of (b) was shown in figure 3-(a) in outer scaling.

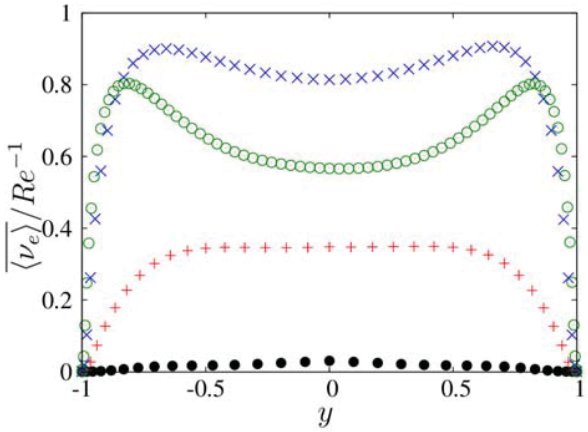

Figure A2. The ratio of the mean eddy viscosity to the kinematic molecular viscosity. The definition of symbols is the same as in figure A1.

[8] Viswanath D 2007 *J. Fluid Mech.* **580** 339–358
[9] Gibson J F and Brand E 2014 *J. Fluid Mech.* **745** 25–61
[10] Brand E and Gibson J F 2014 *J. Fluid Mech.* **750** R3
[11] Rawat S, Cossu C, Hwang Y and Rincon F 2015 *J. Fluid Mech.* **782** 515–540
[12] Deardorff J W 1970 *J. Fluid Mech.* **41** 453–480
[13] Moin P and Kim J 1982 *J. Fluid Mech.* **118** 341–377
[14] Mees A I 1981 *Dynamics Of Feedback Systems* (New York, Wiley)
[15] Saad Y 2003 *Iterative Methods for Sparse Linear Systems* 2nd ed. (SIAM)
[16] Shimizu M and Kawahara G 2014 *Euromech Coll.* **565**, Cargese, FR
[17] Toh S and Itano T 2003 *J. Fluid Mech.* **481** 67–76
[18] Peixinho J and Mullin T 2007 *J. Fluid Mech.* **582** 169–178
[19] van Veen L and Kawahara G 2011 *Phys. Rev. Lett.* **107** 114501
[20] Avila K, Moxey D, Lozar A, Avila A, Barkley D and Hof B 2011 *Science* **333** 192–196
[21] Pirozzoli S, Barnardini M and Orlandi P 2014 *J. Fluid Mech.* **758** 327–343
[22] Avsarkisov V, Hoyas S, Oberlack M and Garcia-Galache J P 2014 *J. Fluid Mech.* **751** R1